
LARGE SAMPLE NAA FACILITY AND METHODOLOGY DEVELOPMENT

C. ROTH, D. GUGIU, D. BĂRBOS, A. DATCU, L. AIOANEI, D. DOBREA, I. E. ȚĂROIU
VIȘAN, A. BUCȘĂ, A. GHINESCU

Institute for Nuclear Research Pitesti, Romania e-mail: csaba.roth@nuclear.ro

ABSTRACT

A Large Sample Neutron Activation Analysis (LSNAA) facility has been developed at the TRIGA- Annular Core Pulsed Reactor (ACPR) operated by the Institute for Nuclear Research in Pitești, Romania. The central irradiation cavity of the ACPR core can accommodate a large irradiation device. The ACPR neutron flux characteristics are well known and spectrum adjustment techniques have been successfully applied to enhance the thermal component of the neutron flux in the central irradiation cavity. An analysis methodology was developed by using the MCNP code in order to estimate counting efficiency and correction factors for the major perturbing phenomena. Test experiments, comparison with classical instrumental neutron activation analysis (INAA) methods and international inter-comparison exercise have been performed to validate the new methodology.

Key words: (neutron activation analysis, irradiation device)

Introduction

The NAA is a suitable technique for elemental composition analysis. The application on large sample needs a suitable irradiation device and involves the knowledge of the neutron field perturbation and the gamma ray counting efficiency. The “Large Sample” could be defined as a sample in which neutron flux and gamma-ray attenuation can not be neglected, as well the counting efficiency knowledge for the specific sample form is required.

The ACPR-TRIGA is a pulsed reactor, operated since 1980 by the Institute for Nuclear Research from Pitești, Romania. Its core is placed into the pool, by the 14 MW_{th} steady-state TRIGA core. The main feature of the core is a 9" diameter central dry experimental tube. Various experiments can be performed in the cavity by exposure either to a fast neutron fluency of 10¹⁵ n/cm² in a single pulse (20000 MW), or to a fast neutron flux density up to 10¹³ n/cm²s in steady-state operation mode. The reactor is capable of continuous steady-state operation at power levels up to 500 kW, limited by the cooling possibilities of natural convection. The central tube rises up to the water surface, but, for relatively small experimental devices, the offset tube is useful for access and instrumentation.

Prior to the irradiation device design, a consistent characterization of the neutron field in the experimental channel has been performed.

Irradiation device

The neutron flux density and the neutron spectrum in the ACPR central dry channel have been evaluated by Monte Carlo computations, as well as by foil activation measurements followed by spectrum unfolding. The integral flux measured value is 2.4×10^{12} n/cm²s normalized at 100 kW reactor power. The fast neutrons contribution is significant, representing 27% from the integral flux density ($E > 1$ MeV).

In order to increase the weight of the thermal neutrons, few spectrum adjusters have been studied. Water and high density polyethylene cylindrical shielding have been considered. The highest efficiency as supplementary moderator is obtained using 6 cm thick polyethylene shielding, but the useful space for the sample is strongly reduced.

Based on the neutron characterization results, including the spectral adjuster efficiency assessment, an adequate irradiation device has been designed and manufactured. The equipment consists of two major parts: the irradiation device and the measurement device. The irradiation device (**Figure 1**) is a 4 cm thick cylindrical polyethylene vessel, 14 cm inner diameter and 28 cm high. Additional polyethylene layers could have been inserted to increase the shield wall thickness up to 6 or 8 cm. However, MCNP calculations showed no additional benefit in neutron flux softening, because thermal neutrons absorption by the additional polyethylene layer counteracts the neutron flux thermalization effect.

The measurement device is a classical scanning device which allows the controlled movement of the sample in front of the detector (rotation and vertical translation). The gamma detector is protected for the natural background by a cylindrical lead shielding (**Figure 2**).



Figure 12 Irradiation device



Figure 13 Measurement device

The irradiation device neutron field characterization has been performed for the standard configuration of the irradiation device, namely 4 cm thick polyethylene screen, using the multi-foil activation technique [1]. The guess spectrum has been computed using the MCNP code.

The measured neutron spectrum (SAND II output) is presented in **Figure 3**. The integral flux measured value is $2.06 \cdot 10^{12}$ n/cm²s normalized to 100 kW reactor power.

Cross section library for NAA applications

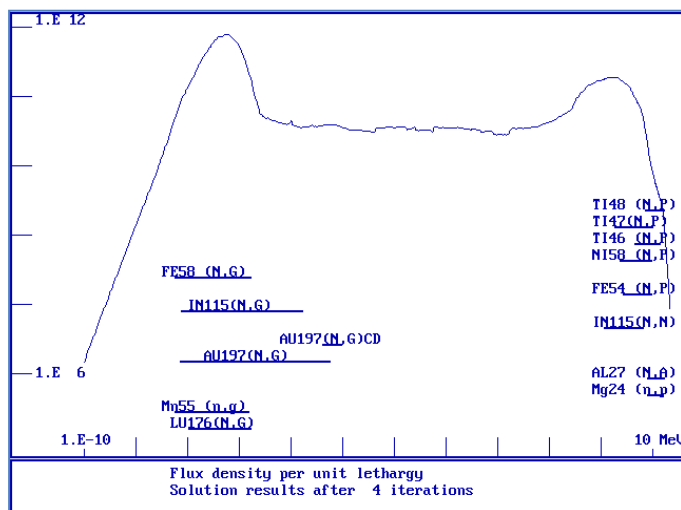


Figure 14 Irradiation device neutron spectrum

A cross section library for NAA applications, specifically for the irradiation device, has been assembled. The mean value of neutron cross sections for each isotope of interest was computed by using the measured neutron spectrum (621 points SAND-II output solution spectrum).

Because the usual dosimetry files (e.g., IRDF[2]) do not contain all reactions of interest for NAA applications, cross sections extracted from the ENDF (Evaluated Nuclear Data File)[3] have been added for all reactions of interest in NAA applications. The differential cross sections have been written in the SAND-II[4] 621 point energy mesh ($10^{-10} - 18$ Mev) using interpolations and/or extrapolations (CSTAPE program[4]) of the

ENDF data. These data, written in the SAND-II cross section library format, are now available for about 200 (n, γ) reactions (almost all neutron capture reaction of the stable isotopes).

A different procedure has been applied for certain cross sections, originated from ENDF, for which the unsolved resonance region is given in a very fine energy mesh (tens of thousands points). Prior to the interpolation/extrapolation these data have been collapsed assuming a $1/E$ neutron energy distribution for the resonance region (intermediate energies). This is a valid assumption for the fission reactor neutron energy distributions. Figure 4 illustrates the results of this procedure for the $^{50}\text{Cr}(n,\gamma)$ reaction cross section.

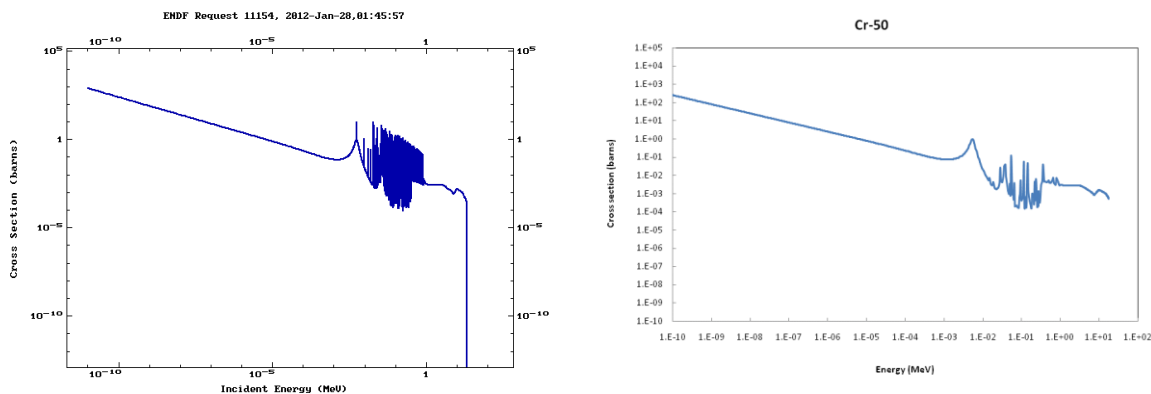


Figure 15 $^{50}\text{Cr}(n,\gamma)$ reaction cross section

Neutron self-shielding effects on large samples

The magnitude of the neutron self-shielding effect has been estimated using MCNP computation. The self-shielding factor is expressed as the ratio of the mean value of the neutron flux over the sample volume when the sample is in place, divided by the same variable without the sample. The computations have been carried out for the typical neutron energy distribution of the ACPR central channel. A cylindrical vessel having the typical pottery composition has been considered as generic sample.

The results presented in **Table 1** show that the magnitude of the self-shielding effect does not exceed few percentage points (it was noticed that the effect increases with the sample density and also with the sample thickness). Therefore, the correction factor for neutron self-shielding effect can be neglected in the present investigation stage, because of its small value (for $\rho=1.8 - 2.3 \text{ g/cm}^3$ the perturbation is less to 1%).

Table 1 Neutron self-shielding evaluation

| Sample description | Neutron spectrum | Neutron self-shielding factor | | |
|----------------------------------|---|-------------------------------|---------------------------|----------------------------|
| | | $\rho=4.8 \text{ g/cm}^3$ | $\rho=2.3 \text{ g/cm}^3$ | $\rho=1.84 \text{ g/cm}^3$ |
| Pottery, cylindrical 5 mm thick | ACPR with spectrum adjuster (6 cm thick polyethylene) | 0.981 | 0.994 | 0.997 |
| Pottery, cylindrical 10 mm thick | | 0.964 | 0.988 | 0.991 |
| Pottery, solid cylinder | | 0.920 | 0.963 | 0.972 |

Counting efficiency evaluation

The efficiency calibration in the gamma spectrometry is performed usually experimentally by a comparative method using a calibration standard source. The preparation of representative calibration standards covering a wide range of materials and forms is difficult. Instead, the use of numerical techniques for detection efficiency computation for large and inhomogeneous samples represents a well accepted solution. The general purpose Monte Carlo code MCNP is a well suited tool for radiation transport simulations. Specific areas of application include detectors design and analysis. The code allows a realistic modeling of any experimental setup (material composition and geometry) taking also into account the most important surrounding objects (shielding, supports) which could affect the counting efficiency. The accuracy of the Monte Carlo simulations of the germanium detector response depends strongly on the detailed information regarding the geometry and the materials used by the manufacturer.

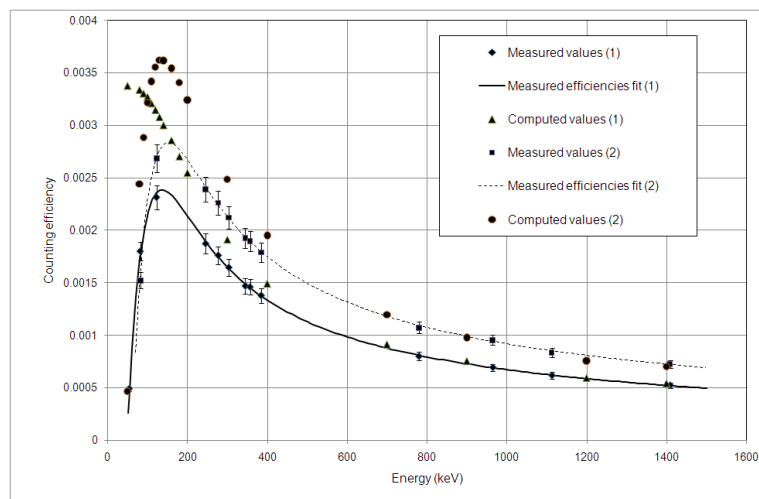


Figure 16 Comparison of computed and measured efficiencies using the modified detector models for point-like sources

In the first stage the detector models provided by the manufacturer have been implemented and comparisons of computed and measured efficiencies for point-like sources and Marinelli geometry have been performed. The results show high discrepancies, especially in the low energy region. For all cases the computed values exceed the measured efficiencies: at high energies ($E > 200 \text{ keV}$) the computed values are higher than the measured values about 15 – 20%; bellow 200 keV the discrepancies increase up to 50% and more. In order to improve the

fitness of the computed efficiencies to the experimental data some step by step adjustments of the detector models have been performed. Two parameters have been modified: the germanium density which affects especially the high energy region and the dead layer thickness affecting the low energy region. After few computational trials an optimal combination of the parameters has been fixed: a lower density value and a 100% increase of the dead layer thickness (from 700 μm to 1400 μm). Acceptable fitness of the measured data was obtained in the high energy region ($E > 200 \text{ keV}$). **Figure 5** shows the results obtained using the modified detector models for point-like sources efficiencies.

The interest energy range has been limited at 200 keV.

The counting efficiency for the actual pottery sample having an irregular form has been evaluated using the modified detector model. The samples (irregular geometries) have been “split” into pieces which allowed a more accurate simulation of their actual shapes using the capabilities of the MCNP code (arbitrary polyhedra or various conical and cylindrical surfaces). The samples (gamma sources) have been simulated using the “cookie-cutter cell in the source” (CCC) capability of the MCNP code. It allows a uniform distribution of the gamma source in the irregular volumes of the samples. Attention should be paid to the efficiency criterion (EFF) applied for cookie-cutter cell rejection; if in any source cell or cookie-cutter cell the acceptance rate is too low, the problem is terminated for inefficiency. The default value of EFF is 0.01 and it generally lets a problem go by a rather low efficiency, but in some cases an even lower value should be specified.

An energy dependent multiplicative correction factor, obtained by fitting the measured/computed efficiency ratio mean values, has been applied on the computed efficiencies.

Figures 6 and **7** show the equivalence between the actual sample geometry and the simplified computational model considered for MCNP5 simulations (domestic archaeological sample and inter-comparison exercise sample).

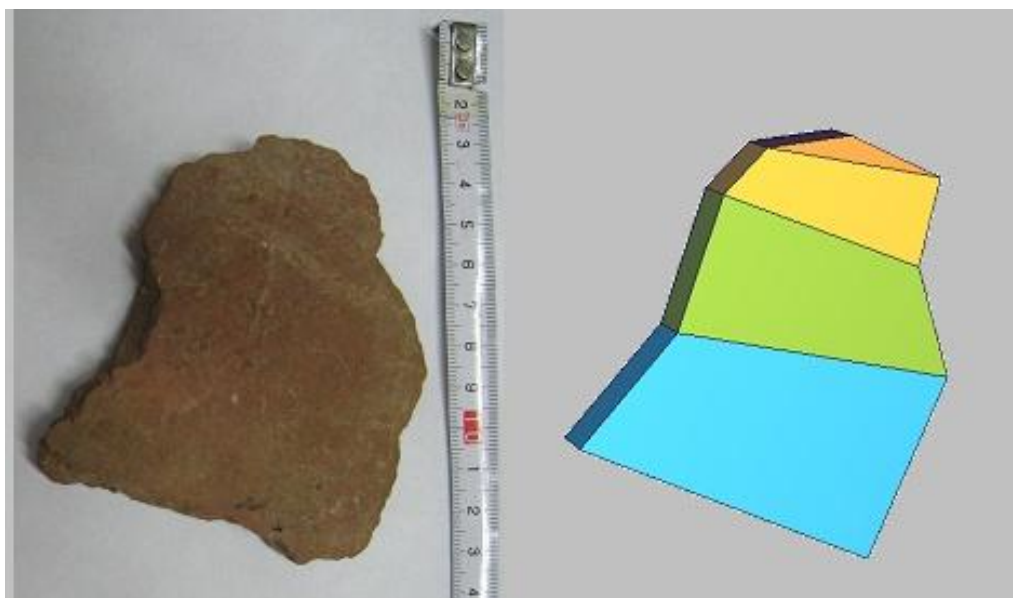


Figure 17 Pottery archaeological sample and MCNP model



Figure 18 IPEN inter-comparison exercise sample and MCNP model

Test irradiations and measurements on pottery samples

The test program has been projected as a comparative study on archaeological and other pottery samples by using the new facility and methodology as well as classical NAA methods. Pottery samples from the “Lumea Noua” neolithic and eneolithic settlement [5] and recent ceramic pots have been selected for investigations.

About 300 mg of powder were sampled from each pottery pieces and then the elemental composition was determined by classical NAA method (k_0 with gold monitor). The powder samples have been exposed in the TRIGA steady state core beryllium reflector ($\Phi_{th}=1.07 \times 10^{13} \text{ cm}^{-2} \text{ s}^{-1}$) respectively in the ACPR core (steady-state operation) using the pneumatic transfer system ($\Phi_{th}=1.06 \times 10^{12} \text{ cm}^{-2} \text{ s}^{-1}$).

The samples have been exposed in the new irradiation device placed in the TRIGA-ACPR core central channel. Gold activation foil detectors have been also placed on the samples. Such detectors (1% or 5% gold in aluminum) are suitable for flux monitoring (appropriate decay and activation). Several gold foil detectors (2 up to 5) have been placed on each sample.

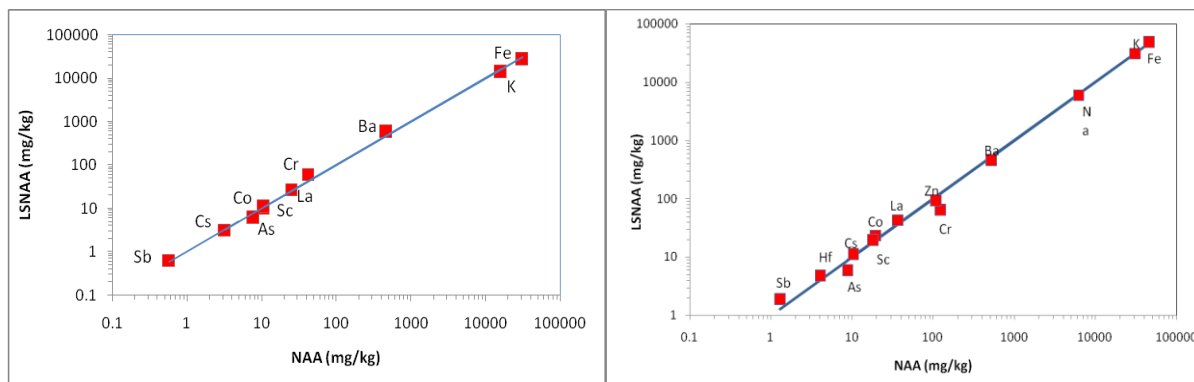


Figure 19 INAA & LSNA results (archaeological pottery samples and pottery vessels)

Figure 8 shows the comparison of INAA and LSNA results for the archaeological pottery samples and pottery vessels used for investigations. The LSNA results show an acceptable agreement with the NAA results, considered as reference.

The main experimental test aimed to validate the methodology developed at the TRIGA-ACPR Reactor has been the inter-comparison exercise performed in the frame of the IAEA coordinated research project using a replica of a ceramic archaeological artefact provided by IPEN (Peru).

The sample has been instrumented with 10 gold flux monitors placed in different position (inside and outside) as well one Lu-Al alloy wire (4.38% Lu) placed along the central vertical axis. The sample the flux density distribution and the mass distribution are presented in **Figure 9**. The axial distribution is normalized to the absolute flux values obtained from gold foil measurements. Taking into account the mass distribution, the weighted mean value of the neutron flux has been computed. The vertical mass distribution has been estimated using the MCNP sample model. The flux density mean value has been $6.62 \cdot 10^{11} \text{ n/cm}^2\text{s}$. The result shows that even we do not obtain a uniform neutron field (otherwise difficult to obtain for large sample), there are possibilities to evaluate the real exposure for sample with non-uniform mass distribution.

Numerical results, presented in **Table 2**, are now subject of the inter-comparison exercise evaluation and will be discussed and analyzed in a separate paper.

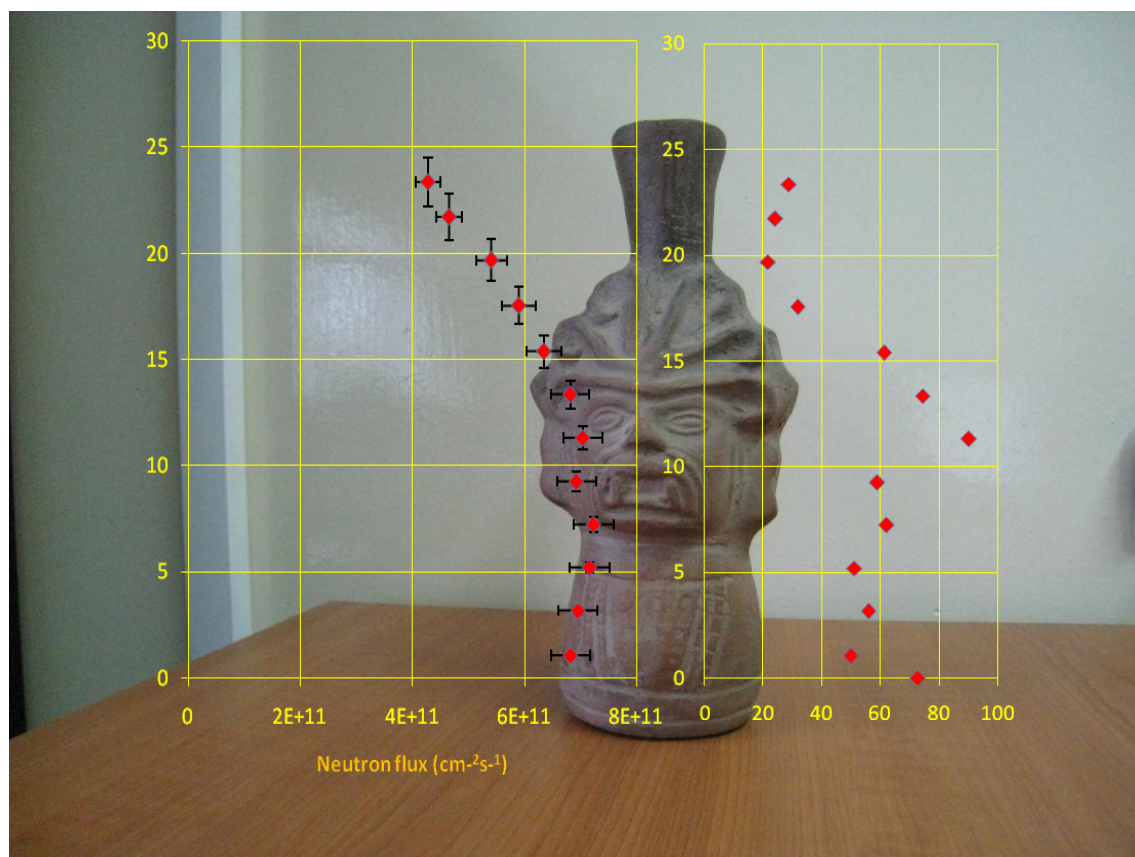


Figure 20 IPEN sample (flux and mass distribution)

Table 2: Inter-comparison exercise results

| Element | Concentration (mg/kg) | Element | Concentration (mg/kg) |
|---------|------------------------|---------|-----------------------|
| La | 26.11 | Hf | 5.17 |
| K | 20339.11 | Zn | 108.42 |
| Na | 19934.53 | Sc | 15.21 |
| Fe | 39914.15 ¹⁾ | Sb | 5.42 |
| | 44069.82 ²⁾ | Rb | 148.46 |
| Cr | 25.2 | Eu | 0.97 |
| Co | 14.23 | Br | 0.76 |
| As | 28.75 | Cs | 11.46 |
| Ba | 627.77 | Mn | 775.7 |

¹⁾⁵⁴Fe(n,p) reaction

²⁾⁵⁸Fe(n,γ) reaction

Uncertainties evaluation

The LSNA is a complex process, involving the sample irradiation, induced activity measurement and data processing as illustrates in **Figure 10**. An accurate assessment of the uncertainty affecting the final result is difficult to be done at moment. However, the main uncertainties may arise from the flux monitoring and the counting efficiency knowledge. 10% uncertainty affecting these values (neutron flux and counting efficiency) may be considered as a reasonable evaluation.

Consequently, uncertainties around 20% affecting the final results may be considered as a realistic estimate, at least at this stage of methodology development.

The counting efficiency assessment for large samples is a complex process involving detector model adjustment in order to fit the experimental data for point-like sources, sample modelling and efficiency curve fitting. The comparison to the standards is made only in the first stage of evaluation (detector model adjustment).

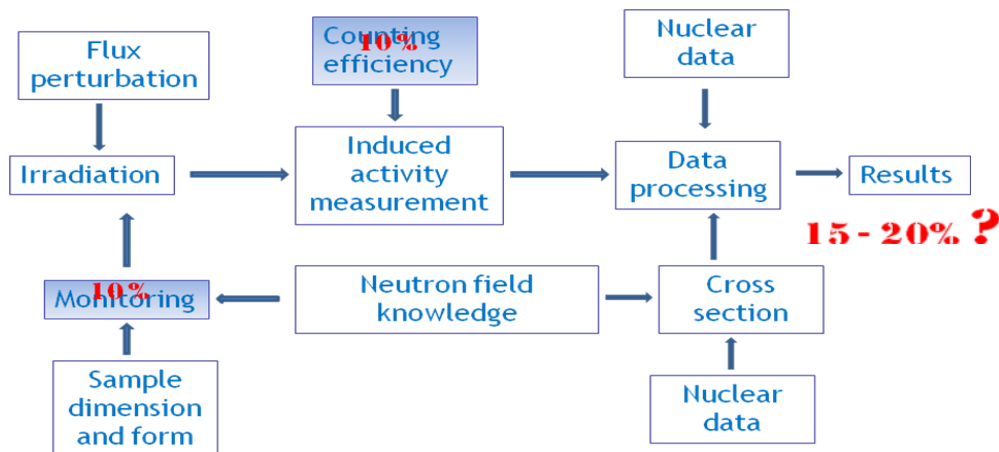


Figure 21 LSNA process diagram

Acknowledgments

The works presented in this paper have been performed in the frame of the IAEA Coordinated Research Project “Large Sample Neutron Activation Analysis Techniques for Inhomogeneous Bulk Archaeological Samples and Large Objects”. We express our acknowledgments for the IAEA financial support and for the high quality and useful technical supervision offered during the Project.

References

- [1] C. Roth, D. Bărbos, D. Gugu, A. Datcu, D. Dobrea, M. Gligor, M. Preda, M.B. Mweetwa - Irradiation and Measurement Devices and Methods Development for LSNA Applications at the TRIGA-ACPR Core, Modern Trends in Activation Analysis – MTAA-13 Conference, Texas A&M University, March 13-18, 2011, published in Journal of Radioanalytical and Nuclear Chemistry, Vol. 291, Issue 2 (2012), 461-466, Doi 10-1007/s10967-011-1231-7
- [2] The International Reactor Dosimetry File: IRDF-2002, www.nndc.bnl.gov/nndcscr/libraries/irdf/
- [3] Evaluated Nuclear Data File (ENDF), National Nuclear Data Center, Brookhaven National Laboratory, www.nndc.bnl.gov/exfor/endl00.jsp
- [4] W.N. McElroy, S. Berg - Spectrum Analysis by Neutron Detectors II and Associated Codes, Techn. Rep. AFWL-TR-67-41, Vol. I, II (1967)
- [5] M. Gligor – Alba Iulia – Lumea Noua Neolithic and Eneolithic Settlement in the Light of Recent Research, Ed. Mega Cluj-Napoca, 2009, ISBN: 978-606-543-045-7